A LASER-INDUCED ULTRASONIC PROBE OF THE MECHANICAL PROPERTIES OF ALIGNED LIPID MULTIBILAYERS

GREGORY EYRING AND M. D. FAYER
Department of Chemistry, Stanford University, Stanford, California 94305

ABSTRACT The recently developed laser-induced phonon spectroscopy (LIPS) technique is applied to the determination of dynamic mechanical properties of aligned dilauroylphosphatidylcholine (DLPC) multibilayer arrays containing 2 and 20% water by weight. Sample excitation by two crossed 100-ps laser pulses generates a longitudinal ultrasonic wave whose wavelength depends on the crossing angle. In these experiments, the acoustic wave propagates parallel to the bilayer planes. The ultrasonic velocity and attenuation are monitored through the diffraction of a variably delayed probe pulse by the acoustic grating. The velocity measures the lateral area compressibility of the bilayers, while the attenuation is related to the viscosity. Velocities obtained in the gel and liquid crystal phases are compared with those found previously using Brillouin scattering. The acoustic attenuation is shown to be an order of magnitude more sensitive to the gel-liquid crystal phase transition than the velocity. The lipid area compressibility and viscosity of DLPC-20% water multilayers with and without 100 mM $CaCl_2$ are found to be identical within our experimental error.

INTRODUCTION

The application of a variety of experimental techniques to lipid-water multibilayer systems has greatly enhanced our understanding of the physical properties of biological membranes. A key method for elucidating the dynamic mechanical properties of these systems has been ultrasonic wave propagation (1–7). Most frequently, such studies are carried out on mutlilamellar vesicles in the presence of excess water. Under these conditions, the measured sound velocity and attenuation are independent of propagation direction; i.e., they are bulk properties. The advent of relatively thick, aligned multilamellar samples (8–10), however, has made it possible to explore the anisotropy of the mechanical properties by choosing the acoustic wave vector to be at an arbitrary angle with respect to the bilayer normal. Using Brillouin light scattering to generate acoustic waves of well-defined wave vector in aligned dipalmitoylphophatidylcholine (DPPC) multilayers, Le Pesant et al. (7) obtained the high frequency elastic constants of this system at a variety of water and cholesterol concentrations.

We describe here the application of a recently developed ultrasonic technique called laser-induced phonon spectroscopy (LIPS) (11, 12) to the study of the mechanical properties of aligned, multilamellar lipid-water phases. In effect, LIPS is the time-domain analogue of Brillouin scattering. However, in several respects LIPS is more flexible in that it is capable of generating acoustic waves of lower frequency ($<10^8$ Hz vs. $>10^9$ Hz) and of accurately measuring large acoustic attenuations.

Briefly, the typical experiment proceeds as follows. The aligned lipid multibilayers are exposed to two crossed, picosecond excitation pulses having the same wavelength and polarization. Constructive and destructive interference in the crossing volume produces a sinusoidally varying pattern of intensity peaks and nulls that launches an acoustic standing wave. The acoustic wavelength and orientation match the interference pattern geometry (11). The periodic density (and thus refractive index) variations associated with the acoustic wave propagation act as a diffraction grating for a variably delayed probe pulse incident at the Bragg angle. The changes in diffracted probe intensity as a function of delay time following the grating excitation are used to calculate the velocity and attenuation of the induced ultrasonic wave (12).

LIPS has previously been used to explore the mechanical properties of a variety of bulk liquids and solids (11, 12), and recently it has been extended to the isotropic, nematic, and smectic A phases of thin liquid crystal films (13). Here we report LIPS data on smectic multi-bilayer arrays of dilauroylphosphatidylcholine (DLPC) containing 2% water by weight in both the liquid crystal and gel phases. From the velocity and attenuation of 200–600-MHz longitudinal waves propagating parallel to the bilayer planes, the lateral area compressibility and viscosity of the bilayers are calculated. These values are compared with those obtained previously on the DPPC-water

system (7). Also, we report preliminary results on the effect of 100 mM $CaCl_2$ on the mechanical properties of DLPC multibilayers containing 20% water by weight. LIPS enjoys several unique advantages over other ultrasonic techniques, and further experiments are outlined in which these will be used to explore the mechanical properties of these model membranes in a variety of physical and chemical environments.

THEORY

The longitudinal acoustic wave launched in the multibilayer samples in response to the grating excitation is due to both thermal and electrostrictive perturbations of the density. Under these conditions the time dependence of the diffracted probe intensity is given by (12):

$$I(t) \propto \{A[1 - \cos \omega t \cdot \exp(-\alpha V t)] - B[\sin \omega t \cdot \exp(-\alpha V t)]\}^2, \quad (1)$$

where A and B are constants specifying the amplitudes of the thermal and electrostrictive contributions, respectively, and ω is the circular frequency of the acoustic wave having velocity V and attenuation α (neper [Np]/cm). In lipids the thermal term dominates for 1.06 - μm excitation ($A > B$), although the electrostriction term is not negligible and must be included to analyze the data properly. The heating is due to absorption by the forbidden $v = 0 \rightarrow v = 3$ vibrational transition of C-H stretching modes, followed by rapid radiationless relaxation. The heating occurs in the intensity peaks of the optical interference pattern and launches an acoustic wave having the grating wavelength. We estimate that the temperature increase in the intensity peaks is $<10^{-3}$ °K per shot. Thus, the excitation of the acoustic wave is an extremely mild perturbation of the sample. Note that for times $t \gg (\alpha V)^{-1}$, $I(t) \propto A^2$, reflecting the fact that after the acoustic waves have been damped or have propagated out of the grating region, a temperature grating remains that decays with the thermal diffusion time (microseconds). In the lipid multilayers $(\alpha V)^{-1}$ is of order 10^{-8} s. Thus, on a nanosecond time scale, the diffraction intensity tends to a constant nonzero value.

The two observables in an ultrasonic experiment are the acoustic velocity V and attenuation α. The acoustic velocity is related to the elastic constants C_{ij} of the system, while the attenuation reflects relaxation processes that tend to absorb the acoustic energy. Following Le Pesant et al. (7), we note that the lipid-water multilayer system is characterized by three elastic constants, denoted C_{11}, C_{33}, and C_{13}, and the system can support two acoustic waves with speeds V_1 (transverse) and V_3 (longitudinal). We have

$$v_1^2 + v_3^2 = \rho^{-1}[C_{11} + (C_{33} - C_{11}) \cos^2 \psi];$$
$$v_1^2 v_3^2 = \rho^{-2}[C_{11}C_{33} - C_{13}^2] \sin^2 \psi \cos^2 \psi, \quad (2)$$

where ρ is the macroscopic density and ψ is the angle between the acoustic wave vector and the normal to the bilayers. Here $\psi = 90°$ (wave vector in the plane of the bilayer) so that:

$$v_1^2 = 0$$

and

$$v_3^2 = \rho^{-1} C_{11}. \quad (2a)$$

The elastic constant C_{11} is a measure of the area compressibility of the lipid in the bilayer plane at constant layer spacing d:

$$C_{11} = -A\left(\frac{\partial P}{\partial A}\right)_d = \rho\left(\frac{\partial P}{\partial \rho}\right)_d, \quad (3)$$

where A is the area per molecule and P is the lateral pressure that tends to change A. It is implicit that the derivatives are taken at constant entropy and water concentration (7).

The acoustic attenuation α can be written as the sum of three contributions (14):

$$\alpha = \alpha_\eta + \alpha_i + \alpha_c, \quad (4)$$

where α_η represents absorption due to viscous effects; α_i, the absorption due to acoustic perturbations of the lipid internal degrees of freedom; and α_c, the attenuation caused by critical fluctuations near phase transitions. Both α_i and α_c are dynamic quantities that are associated with specific relaxation processes having characteristic times τ_i. The contribution of these terms to the overall acoustic absorption is therefore strongly dependent on the frequency $\omega = 2\pi f$ (14):

$$\alpha/f^2 = B^\infty + \sum_i A_i^0 \tau_i (1 + \omega^2 \tau_i^2)^{-1}. \quad (5)$$

B^∞ is a constant that describes the limiting viscosity at high frequency, and A_i^0 is proportional to the volume viscosity at zero frequency of process i. Gamble and Schimmel (4) fit their ultrasonic absorption data on the gel-liquid crystal transition in DPPC vesicles approximately with a single relaxation time τ = 10 ns (16 MHz). This was attributed to acoustic absorption associated with rotational isomerization about carbon-carbon single bonds of the lipid chains, a process that is strongly coupled to the phase transition. They did not observe any significant relaxation processes above 150 MHz. In the work described here, typical acoustic frequencies are in the range 200–600 MHz. Therefore, with $\omega^2\tau^2 \gg 1$ we can neglect the second term in Eq. 5 and obtain:

$$\alpha/f^2 = \alpha_\eta/f^2 = B^\infty. \quad (5a)$$

Just as with the acoustic velocity, the symmetry of the multibilayer array requires that the attenuation be anisotropic; i.e., its magnitude depends on the acoustic wave vector (15). For the case of $\psi = 90°$, the expression for α/f^2 simplifies to (14):

$$\alpha/f^2 = \frac{2\pi^2}{\rho V^3}(\eta_2 + \eta_4), \quad (6)$$

where η_2 and η_4 are two of the five viscosities required to describe a compressible smectic system, in the notation of reference 15. If we identify η_2 with the shear viscosity η and $\eta_4 = \eta' + \frac{1}{3}\eta$ where η' is the bulk or volume viscosity, this reduces to the equation describing ultrasonic attenuation in an isotropic liquid (14):

$$\alpha/f^2 = \frac{2\pi^2}{\rho V^3}(4/3\eta + \eta'), \quad (7)$$

EXPERIMENTAL PROCEDURES

The laser system used in these experiments is a continuously pumped Nd/YAG oscillator that is acousto-optically mode-locked and Q-switched to produce 1.06-μm pulses at 200 Hz (11). The output is a train of some 40 mode-locked pulses of width ~100 ps separated by 11 ns. A ~50-μJ pulse from the center of the train is selected out by a Pockels cell. A small portion of the infrared (IR) single pulse is frequency doubled using CD*A to give a ~5-μJ probe at 532 nm. The remainder is beam split to give two ~15-μJ pulses that, after traveling equal path lengths, are crossed at an angle θ in the sample (Fig. 1). The sample is thus exposed to a sinusoidally varying pattern of intensity peaks and nulls produced by the interference between the IR excitation beams. The fringe spacing Λ is given by:

$$\Lambda = \frac{\lambda}{2 \sin(\theta/2)}, \quad (8)$$

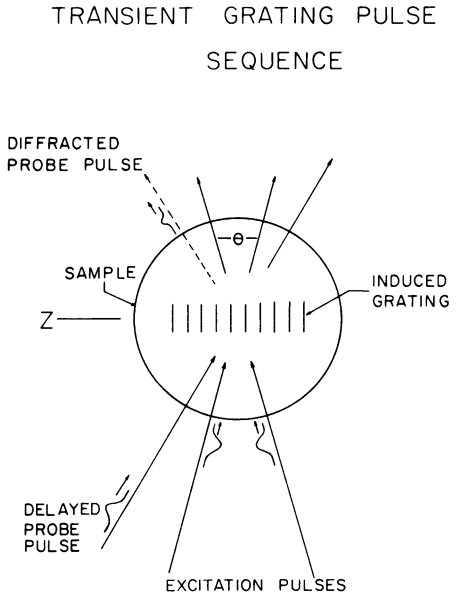

FIGURE 1 Schematic illustration of the LIPS experiment. The crossed excitation pulses generate a standing longitudinal acoustic wave in the aligned lipid multibilayers having the wavelength and orientation (wave vector along Z) of the optical interference pattern. The resulting time-dependent modulation of the index of refraction creates a diffraction grating that Bragg-diffracts a variably delayed probe pulse. In this case, Z is parallel to the bilayer planes.

where λ is the laser wavelength. In this work, Λ was kept constant at 3.8 μm.

The interaction region of the IR excitation beams is probed at the Bragg angle with the 532-nm pulse that could be timed to arrive continuously from 1 ns before to 16 ns after the IR excitation, using an optical delay line. Spot sizes of the excitation and probe beams were 100 and 60 μm, respectively. The probe diffraction was detected with a photodiode coupled to a lock-in amplifier, and signal from each scan of the optical delay line was stored on a computer for subsequent analysis.

The lipid DLPC was obtained from Avanti Polar Lipids, Inc. (Birmingham, AL) and was lyophilized from benzene after filtration through a pore size of 0.1 μm to remove dust particles (16). Appropriate quantities of water were added externally with a microliter syringe, and the mixtures were allowed to equilibrate for several days before use. Approximately 10–20 mg of the lipid-water mixture was sandwiched between silica optical flats separated by a Teflon spacer of 125 or 280-μm thickness. The surfaces of the flats had been treated with octadecyltrichlorosilane (Petrarch Systems Inc., Levittown, PA), which is known to produce homeotropic alignment (director perpendicular to the surface) of liquid crystal films (17). This assembly was inserted into a variable temperature cell that could be heated resistively up to 200 °C. The temperature was monitored using a 3-mm platinum resistance thermometer (GSO 330; Omega Engineering, Inc., Stamford, CT) that was inserted into a hole drilled into one of the optical flats. The temperature was constant to ±0.2 °C.

Alignment of the sample into planar, multibilayer arrays was achieved by gently shearing and compressing the lipid above the gel-liquid crystal phase transition temperature, according to the method of Asher and Pershan (10). The process was monitored by placing the sample on the stage of a polarizing microscope, in which the aligned regions appear black between crossed polarizers. DLPC samples 125-μm thick containing 20% water by weight could be aligned at room temperature, with monodomain regions several square millimeters in area obtained after ~20 min (10). In samples containing 2% water by weight, monodomain regions 280-μm thick were obtained by the same method after first heating the lipid to 125 °C. The uniaxial alignment of the liquid crystalline phase was preserved after slow cooling (~1 °C/min) until at 40 °C the phase transition to the biaxial gel occurred. This could be detected either as an increase in light transmission through the sample viewed with a polarizing microscope, or as an increase in the scattering of the probe laser beam. Extensive optical studies of the DPPC-water phase diagram have been carried out (9) showing the strong dependence of the phase transition temperature on water concentration in these multilayer systems.

The data were least-squares fit to Eq. 1 with the four parameters A, B, α, and ω. The velocity V is obtained from

$$V = \frac{\Lambda\omega}{2\pi} \tag{9}$$

and typically is accurate to ±1%. The uncertainty in the acoustic attenuation was estimated from repeated sets of data to be ±7%. Because the four parameters are nearly independent of one another, we found that the fitting procedure always yielded the same final values, regardless of the initial guesses.

RESULTS AND DISCUSSION

Typical LIPS data from 280-μm thick DLPC multibilayers containing 2% water by weight (~1:1 molar ratio) are shown in Fig. 2. At $t = 0$, the excitation and probe pulses are all simultaneously inside the sample. The small peak at $t = 0$ is due to diffraction from the electronic Kerr effect (18), which disappears with the cross correlation time of the excitation and probe pulses (13). After $t = 0$, the probe diffraction rises and falls with the periodic modulation of the density caused by a longitudinal acoustic standing wave propagating parallel to the bilayer planes.

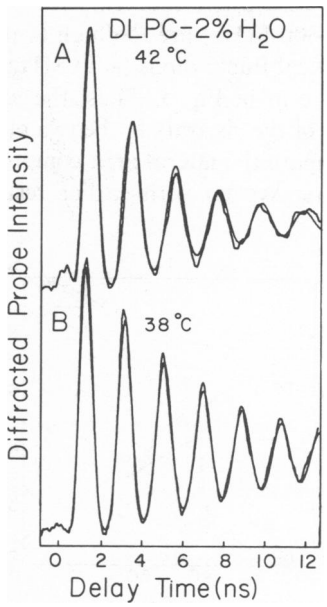

FIGURE 2 The diffracted probe intensity as a function of probe delay time in the liquid crystal phase (A) and gel phase (B) of 280-μm thick aligned DLPC multibilayers containing 2% water by weight. The phase transition temperature T_c is 40°C. Also shown is the least-squares fit of the data to Eq. 1, which yields the acoustic velocity V and attenuation α. In A, $V = 1.82 \times 10^5$ cm/s and $\alpha/f^2 = 560 \times 10^{-17}$ s^2/cm. In B, $V = 1.97 \times 10^5$ cm/s and $\alpha/f^2 = 280 \times 10^{-17}$ s^2/cm.

The acoustic period is obtained from the spacing between the diffraction peaks, while the attenuation is found from the exponentially decreasing peak amplitudes (12). In Fig. 2 *A*, the temperature is 2 °C above the gel-liquid crystal phase transition at this water concentration (T_c = 40 °C), and in 2 *B*, 2 °C below it. Also shown are least-squares fits of these data to Eq. 1, yielding $A = 0.43$, $B = 0.35$, $V = 1.82 \times 10^5$ cm/s, $\alpha/f^2 = 560 \times 10^{-17}$ s²/cm in the liquid phase; and $A = 0.37$, $B = 0.09$, $V = 1.97 \times 10^5$ cm/s, $\alpha/f^2 = 280 \times 10^{-17}$ s²/cm in the gel phase. It is found that $A > B$, i.e., the heating mechanism is the dominant means by which the acoustic waves are generated. This dominance is magnified by the fact that the constant A multiples a $(1 - \cos \omega t)$ term that at its maximum is twice as large as the $\sin \omega t$ term multiplied by B. The quantity α/f^2 is reported rather than α because at high frequencies $\alpha \propto f^2$ (Eq. 5a). This facilitates the comparison of attenuations measured at different frequencies.

Fig. 3 displays the temperature dependence of the acoustic velocity and attenuation for the same sample and propagation direction as in Fig. 2. The gel-liquid crystal phase transition is observed at 40 °C as an abrupt change of ~8% in the acoustic velocity and of nearly a factor of two in the attenuation. Thus, the attenuation is more sensitive to the physical state of the membrane than the velocity. The slope of the velocity vs. temperature curve appears to be the same in the gel and liquid crystal phases, and this seems to hold for the attenuation as well. The fact that no anomalous increases in the attenuation or decreases in the velocity are observed at the phase transition (5) is consistent with the conclusion that the acoustic frequencies involved (200–600 MHz) are too high to permit effective coupling to critical fluctuations (~20 MHz) (4) described in the second term in Eq. 5. Thus, the attenuation is a direct measure of the viscosity in the two phases (Eq. 6).

We can compare the lateral area compressibility of the DLPC-2% water system with earlier results on DPPC-2.5% water obtained by Brillouin scattering (7). To take account of the fact that the phase transition temperature T_c in the DPPC system is much higher (~80 °C as compared with 40 °C), we consider the elastic constants as a function of $\Delta T = (T - T_c)$ in the gel phase. For $\Delta T = -10$ °C, we obtain from Fig. 3 and Eq. 2a $\rho^{-1} C_{11} = 4.24 \times 10^{10}$ cm²/s² for DLPC as compared with 3.5×10^{10} cm²/s² for DPPC. At $\Delta T = -20$ °C, we find in DLPC 4.75×10^{10} cm²/s², while in DPPC the value is 4.1×10^{10} cm²/s². No data were reported in DPPC above T_c at this water concentration (7). Given that the macroscopic density of the DPPC samples is probably 10–20% lower at a given ΔT, we can conclude that the in-plane area compressibilities of the two bilayers are approximately equal, i.e., they are independent of chain length.

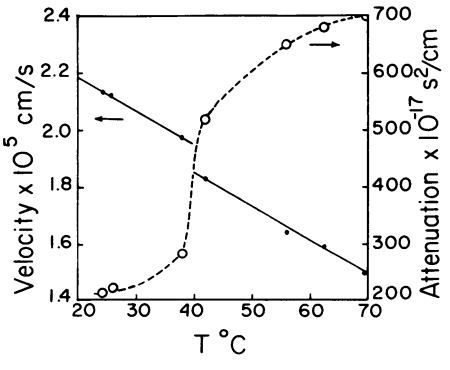

FIGURE 3 The temperature dependence of the ultrasonic velocity (closed circles) and attenuation (open circles) for the same sample as in Fig. 2. At T_c = 40°C, the velocity changes by ~8%, while the attenuation jumps by nearly a factor of 2. Uncertainties for the velocities and attenuations are ±1 and ±7%, respectively. See text for the computation of the elastic constant C_{11} and viscosity η from these data.

The membrane viscosities obtained from ultrasonic attenuation measurements are not directly comparable to those deduced from rotational and translational diffusion studies (19–21) since in the latter the volume viscosity is not considered. However, we can make an approximate comparison using Eq. 6 by noting that in most liquids $\eta_4 \approx \eta_2$ in the high frequency range (14). Taking $\alpha/f^2 \approx 700 \times 10^{-17}$ s²/cm at 70 °C in Fig. 3, we have $(\eta_2 + \eta_4) = 1.2\ \rho$ poise or $\eta \approx 0.6\ \rho$ poise. The reported value for the viscosity of most biological membranes is ~1 poise from diffusion measurements (19–21) in good agreement with our approximate result.

We also examined the mechanical properties of DLPC multilayers containing 20% water by weight. At this water content, which corresponds to half of the maximum possible water uptake, the phase transition temperature is ~0 °C (22). The sample could be aligned at room temperature (10), where $\Delta T = +20$ °C. We obtained $V = 1.57 \times 10^5$ cm/s and $\alpha/f^2 = 430 \times 10^{-17}$ s²/cm, corresponding to $\rho^{-1} C_{11} = 2.46 \times 10^{10}$ cm²/s² and $\eta \approx 0.4\ \rho$ poise. Le Pesant et al. (7) measured $\rho^{-1} C_{11} = 2.2 \times 10^{10}$ cm²/s² at $\Delta T = +20$ °C in DPPC multilayers containing 25–30% water. This once again indicates that the elastic constant C_{11} is independent of chain length, although it depends strongly on water content at low water concentrations (7).

The influence of divalent cations on the properties and interactions of cell membranes has been a subject of active interest. In particular, Ca^{2+} ions have been shown to induce phase transitions and structural rearrangements in bilayers containing charged lipids like phosphatidylserine (23). Recently, however, it has been recognized that Ca^{2+} also adsorbs onto zwitterionic phosphatidylcholine head groups (24, 25). This results in increased separation between bilayers in nonaligned multibilayer samples, as well as phase separation in bilayers made up of lipid mixtures (25). For example, at room temperature 1 mM $CaCl_2$ causes the separation between DPPC bilayers, determined by x-ray scattering, to increase from 19 Å inpure water to > 90 Å (24).

To explore the effect of Ca^{2+} ions on the mechanical properties of the DLPC bilayers, we aligned a 125-μm

thick sample containing 20% by weight 100 mM $CaCl_2$ solution. The acoustic velocity and attenuation at $\psi = 90°$ were compared with those of an identical sample hydrated with 20% pure water. Within our experimental error, the 100 mM Ca^{2+} did not cause a change in either of the measured values. There could be several explanations for this result. One possibility is that there were insufficient numbers of Ca^{2+} per head group (~1:64) to significantly perturb the multilayer structure. Our sample differed from those studied previously in that the quantity of calcium ions was fixed at the outset by the amount of solution used to hydrate the DLPC, rather than having the lipid in equilibrium with a bath of excess Ca^{2+} at a given concentration. However, the 1:64 ratio is in the range examined in the x-ray experiments. Another explanation is that the separation between the multilayers was indeed larger in the presence of Ca^{2+}, but the in-plane bilayer properties were not significantly affected. Further experiments using various $[Ca^{2+}]$ at constant water composition and various water concentrations at constant $[Ca^{2+}]$ should provide valuable information about the influence of Ca^{2+} on bilayer structure and properties.

CONCLUSION

Here we have demonstrated that the LIPS technique, previously applied to study acoustic wave propagation in bulk liquids, solids, and liquid crystals, can be used to explore the mechanical properties of model biological membranes. By measuring the velocity of a longitudinal acoustic standing wave propagating parallel to the bilayer planes, we obtained the lateral area compressibility of DLPC bilayers in the 200–600 MHz range at 2 and 20% water. These values were nearly identical to earlier results in DPPC multilayers from Brillouin scattering measurements above 1 GHz. From the acoustic attenuation, approximate values of the bilayer viscosity were calculated that agreed well with previous values based on rotational and translational diffusion. The gel-liquid crystal phase transition was observed in DLPC-2% water multilayers, and was shown to affect the acoustic attenuation significantly more than the velocity. Finally, the compressibility and viscosity of DLPC-20% water bilayers with and without 100 mM $CaCl_2$ were shown to be identical within our experimental error.

The above experiments were performed using a single acoustic wavelength and propagation direction. By rotating the aligned multibilayer samples with respect to the crossed excitation beams, one can generate a sound wave in any desired direction, permitting the three elastic constants of Eq. 2 to be determined. Also, by reducing the angle between the beams, the wavelength can be increased (Eq. 8), and thus the frequency reduced to the range in which the acoustic wave can couple to the lipid internal degrees of freedom and to fluctuations of the order parameter near the phase transition (~20 MHz). In this range, the dispersion in the velocity and attenuation provides information on dynamic relaxation processes in the bilayers, rather than on the viscosity alone.

In several respects, the LIPS technique combines the most desirable characteristics of the two ultrasonic methods that have previously been applied to lipid studies. As with Brillouin scattering, the acoustic frequency and wave vector can be continuously varied. As with transducer techniques, the frequency can be reduced to the chemically interesting megahertz range, and large attenuations can be conveniently measured. Thus, the application of LIPS to lipid multilayer systems containing varying amounts of water, ions, cholesterol, and other biological ingredients is a fruitful source of information on the mechanical properties of biological membranes.

M. D. Fayer would like to thank the Guggenheim Foundation for fellowship support that contributed to this work.

This work was supported by a grant from the National Institutes of Health (No. GM32205). Equipment used in the experiments was provided by the National Science Foundation (No. DMR 79-20380).

REFERENCES

1. Hammes, G. G., and P. B. Roberts. 1970. Ultrasonic attenuation measurements in phospholipid dispersions. *Biochim. Biophys. Acta.* 203:220–227.
2. Eggers, F., and Th. Funk. 1976. Ultrasonic relaxation spectroscopy in liquids. *Naturwissenschaften.* 63:280–285.
3. Mitaku, S., A. Ikegami, and A. Sakanishi. 1978. Ultrasonic studies of a lipid bilayer. Phase transition in synthetic phosphatidylcholine liposomes. *Biophys. Chem.* 8:295–304.
4. Gamble, R. C., and P. R. Schimmel. 1978. Nanosecond relaxation processes of phospholipid bilayers in the transition zone. *Proc. Natl. Acad. Sci. USA.* 75:3011–3014.
5. Sakanishi, A., S. Mitaku, and A. Ikegami. 1979. Stabilizing effect of cholesterol on phosphatidylcholine vesicles observed by ultrasonic velocity measurement. *Biochemistry.* 18:2636–2642.
6. Mitaku, S. 1981. Ultrasonic studies of lipid bilayer phase transition. *Mol. Cryst. Liq. Cryst.* 70:21–28.
7. Le Pesant, J.-P., L. Powers, and P. S. Pershan. 1978. Brillouin light scattering measurement of the elastic properties of aligned multilamella lipid samples. *Proc. Natl. Acad. Sci. USA.* 75:1792–1795.
8. Powers, L., and N. A. Clark. 1975. Preparation of large monodomain phospholipid bilayer smectic liquid crystals. *Proc. Natl. Acad. Sci. USA.* 72:840–843.
9. Powers, L., and P. S. Pershan. 1977. Monodomain samples of dipalmitoylphosphatidylcholine with varying concentrations of water and other ingredients. *Biophys. J.* 20:137–152.
10. Asher, S. A., and P. S. Pershan. 1979. Alignment and defect structures in oriented phosphatidylcholine multilayers. *Biophys. J.* 27:393–422.
11. Fayer, M.D. 1982. Dynamics of molecules in condensed phases: picosecond holographic grating experiments. *Annu. Rev. Phys. Chem.* 33:63–87.
12. Miller, R. J. D., R. Casalegno, K. A. Nelson, and M. D. Fayer. 1982. Laser-induced ultrasonics: a dynamic holographic approach to the measurement of weak absorptions, optoelastic constants, and acoustic attenuation. *Chem. Phys.* 72:371–379.
13. Eyring, G., and M. D. Fayer. 1985. A picosecond holographic grating approach to molecular dynamics in oriented liquid crystal films. *J. Chem. Phys.* In press.

14. Candau, S., and S. V. Letcher. 1978. Ultrasonic propagation in liquid crystals. *Adv. Liq. Cryst.* 3:167–235.
15. Martin, P. C., O. Parodi, and P. S. Pershan. 1972. Unified hydrodynamic theory for crystals, liquid crystals, and normal fluids. *Phys. Rev. A.* 6:2401–2410.
16. Eyring, G., and M. D. Fayer. 1983. Holographic generation of bubble grating at liquid-glass interfaces and the dynamics of bubbles on surfaces. *Chem. Phys. Lett.* 98:428–432.
17. Cognard, J. 1982. Alignment of nematic liquid crystals and their mixtures. *Mol. Cryst. Liq. Cryst. Supp.* 1:1–77.
18. Sala, K., and M. C. Richardson. 1976. Optical Kerr effect induced by ultrashort laser pulses. *Phys. Rev. A.* 12:1036–1047.
19. Saffman, P. G., and M. Delbrück. 1975. Brownian motion in biological membranes. *Proc. Natl. Acad. Sci. USA.* 72:3111–3113.
20. Koppel, D. E., M. P. Sheetz, and M. Schindler. 1981. Matrix control of protein diffusion in biological membranes. *Proc. Natl. Acad. Sci. USA.* 78:3576–3580.
21. Peters, R., and R. J. Cherry. 1982. Lateral and rotational diffusion of bacteriorhodopsin in lipid bilayers: experimental test of the Saffman-Delbrück equations. *Proc. Natl. Acad. Sci. USA.* 79:4317–4321.
22. Chapman, D. 1975. Phase transitions and fluidity characteristics of lipids and cell membranes. *Q. Rev. Biophys.* 8:185–235.
23. Portis, A., C. Newton, W. Pangborn, and D. Papahadjopoulos. 1979. Studies on the mechanism of membrane fusion: evidence for an intermembrane Ca^{2+}-phospholipid complex, synergism with Mg^{2+}, and inhibition by spectrin. *Biochemistry.* 18:780–790.
24. Lis, L. J., V. A. Parsegian, and R. P. Rand. 1981. Binding of divalent cations to dipalmitoylphosphatidylcholine bilayers and its effect on bilayer interaction. *Biochemistry.* 20:1761–1770.
25. Lis, L. J., W. T. Lis, V. A. Parsegian, and R. P. Rand. 1981. Adsorption of divalent cations to a variety of phosphatidylcholine bilayers. *Biochemistry.* 20:1771–1777.